Halloysite-TiO2 Nanocomposites for Water Treatment

Contributor: Mahmoud Abid, Abdesslem Ben Haj Amara, Mikhael Bechelany

Halloysite nanotubes (HNTs) are clay minerals with a tubular structure that can be used for many different applications in place of carbon nanotubes. Indeed, HNTs display low/non-toxicity, are biocompatible, and can be easily prepared. Moreover, the aluminum and silica groups present on HNTs' inner and outer surfaces facilitate the interaction with various functional agents, such as alkalis, organosilanes, polymers, surfactants, and nanomaterials.

---

1. Extraction and Purification of Natural Halloysite

Natural halloysite clay contains impurities (e.g., kaolin, illite, quartz, feldspar, chlorite, gibbsite, salts, and metals) that greatly influence the nanotube size distribution. Therefore, different purification methods (see below) have been investigated to allow its subsequent modification and use for various applications [1][2][3].

1.1. Sedimentation and Purification

Abid et al. dispersed natural halloysite in deionized water and, after overnight sedimentation, removed the fraction with a diameter >2 μm. They washed the obtained clay five times with deionized water and NaCl, followed by centrifugation. Then, they washed Na^+ HNT with distilled water and centrifuged them until the test in the presence of silver nitrate ($AgNO_3$) was negative. They dried the purified HNT in an oven at 110 °C for 3 h, followed by crushing and sieving [3][4].

1.2. Base-Treated Purification

Zhang et al. described a base-treated purification method that does not require high temperatures. Briefly, they mixed crude halloysite and water and then adjusted the pH to alkaline. After adding a dispersing agent, they stirred the solution at room temperature for 6 h. Finally, they collected the purified HNT by centrifugation or filtration [5].

1.3. Drying and Ball Milling

Sakiewicz and Lutynski dried HNTs at 60 °C and crushed them into particles of a size <10 mm. After ball milling for 20 min, they immersed 400 g of the obtained material in 550 cm^3 of water. After stirring and washing, they ground the resulting slurry in a ball mill with steel balls 1–5 mm in diameter. Finally, they washed the material for 4 h [6].

1.4. Magnetic Separation

To eliminate iron-containing impurities, Sakiewicz et al. proposed a multi-gradient magnetic separation approach to separate aluminum ferric silicate in weak magnetic field conditions [7]. With this method, they could remove heavy magnetic minerals (e.g., Fe_3O_4) that are usually difficult to eliminate. Alternatively, they suggested treating halloysite with hydrochloric acid, which will also remove other metal oxide impurities (e.g., copper, calcium, and titanium oxides) to further improve purification [2].

1.5. Acid Leaching and Ball Milling

Sakiewicz and Lutynski used sulfuric acid leaching to improve purification. After drying at 100 °C for 1 h, they used ball milling to crush the raw material, which was then homogenized, stirred, and washed. This was followed by ball milling (steel balls of 5 to 10 mm in diameter) and washing. Then, they added H_2SO_4 to the slurry for leaching in a reactor at 90 °C for 90 min. After washing and filtering the material to separate the magnetite and non-magnetic fractions, they used slow magnetic separation. Then, they separated the particle fraction with a size <20 μm in a sedimentation column. After filtering and drying, the material was ready for microscope analysis [6].

1.6. Ultrasonic Dispersion

Rong et al. used ultrasound to enhance halloysite dispersibility in the aqueous phase. They sonicated the suspension with an ultrasonic cell disruptor at 100–700 W for 100–1500 s. After sonication, they centrifuged the halloysite suspension in an ultracentrifuge. After discarding the supernatant, they collected the resulting sediments and washed them alternately with water and ethanol (three times/each). Finally, they dried the sediments at 60 °C for 12 h [8].

2. Halloysite-TiO$_2$ Nanocomposites for Water Treatment

Recently, clay has been used to eliminate toxic waste from wastewater. Among these remarkable adsorbents, kaolin shows outstanding adsorption and photocatalytic activity as a support material for semiconductors. Its layered structure and size are considered advantageous for developing non-toxic and low-cost photocatalysts with high catalytic activity and stability [9][10]. The theoretical formula of HNT, as rolled aluminosilicate sheets, is similar to that of kaolinite, with the presence of interlayer water molecules as a distinguishing feature compared to kaolinite [10].

Halloysite-TiO$_2$ nanocomposites can be exploited for different applications, including drug delivery, polymer filler, matrix for photocatalysts, and adsorbents for environmental and biomedical applications. researchers will describe the development of inexpensive and effective HNT-TiO$_2$ nanocomposites with very high absorption capacity to eliminate inorganic and organic pollutants present in water.

Recently, several studies have investigated the photodegradation of dyes, pesticides, and antibiotics present in water using either pristine or modified HNT decorated with TiO$_2$ nanoparticles on their outer surface (**Figure 1**a) or loaded with TiO$_2$ nanoparticles on their inner surface (**Figure 1**b). Additionally, some studies have explored the use of halloysite loaded inside TiO$_2$ nanofibers for the same purpose (**Figure 1c**).
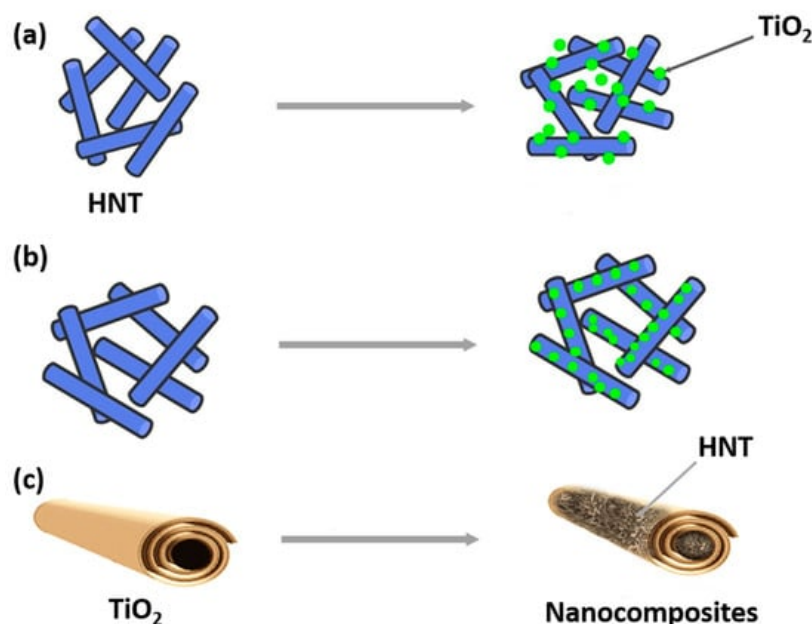

Figure 1. Schematic representation of HNT decorated with TiO$_2$ (**a**), HNT loaded with TiO$_2$ (**b**), and HNT loaded inside TiO$_2$ nanofibers (**c**).

In the last few decades, due to the increase in industrial activities, water pollution has become a major health and environmental issue worldwide [11][12]. Halloysite-TiO$_2$ nanocomposites present great potential for the removal of water contaminants due to their tubular structure, porous surface, low cost, environmental friendliness, and mechanical and chemical resistance.

The nanocomposites that are shown in **Figure 2** can be used to remove dyes from aqueous environments. Dyes are used mostly by the textile and paint industries and are removed by adsorption and/or degradation. Du and Zheng deposited anatase TiO$_2$ on HNT surfaces using calcination at different temperatures (100 to 500 °C) to obtain TiO$_2$-HNT composites. They found that at higher calcination temperatures, the anatase crystalline structure improved, but the HNT structure was damaged at the highest temperature. All tested samples showed very high adsorption capacities that ranged from 38.57 to 54.29 mg/g. The TiO$_2$-HNT composite fabricated at 300 °C could eliminate 81.6% of methylene blue after 4 h of UV irradiation [13]. Rapsomanikis et al. fabricated TiO$_2$/HNT thin films by adding silver using an acetic acid-based sol–gel method. The sample with 20–30% HNT showed higher photooxidation activity (tested by monitoring Basic Blue 41 azo

dye degradation in water under UV irradiation) and better stability than Titania P25 [14]. Similarly, Papoulis et al. showed that the photocatalytic activity of TiO$_2$/HNT (**Figure 2**a) and TiO$_2$/HNT + sepiolite nanocomposites (fabricated with a hydrothermal method at 180 °C) was better than that of Titania P25 (paracetamol, tetracycline, and rhodamine B removal under UV visible light). They explained that this good result was due to the electrostatic attraction forces on the negatively charged HNT surface [15]. Yao et al. assessed the photocatalytic activity of amorphous C + N/TiO$_2$/HNT with different mass ratios (fabricated using the precipitation-dissolution-recrystallization method and calcination at 550 °C for 4 h). After 1 h under natural light, C + N/TiO$_2$/HNT with a mass ratio of 4.5 and TiO$_2$/HNT degraded 95% and 85% of methylene blue, respectively. This difference was explained by the larger BET surface. C + N/TiO$_2$/HNT remained stable after five cycles [16]. Li et al. synthesized 1D-polyaniline (PANI)-TiO$_2$-HNT nanocomposites at different pHs and different volume concentrations with a low-temperature synthesis method. The samples prepared at pH 0.5 and with 1% *v/v* showed the highest photoactivity for rhodamine B degradation due to the PANI sensitizing effect and the charge transfer to TiO$_2$. The PANI-TiO$_2$-HNT photocatalyst degraded 73.49% of rhodamine B (10 mg/L) and was reused four times without loss of photoactivity under visible light. The authors propose that HNT can be used for wastewater treatment [17]. Mishra et al. fabricated a TiO$_2$@HNT photocatalyst by combining sol–gel and phase inversion (**Figure 2**b). This photocatalyst displayed good stability and improved photocatalytic activity due to the electrostatic interaction between TiO$_2$ and the HNT surface. The nanocomposite degraded 87.47% and 96.87% of 20 mg/g methylene blue and rhodamine B, respectively, under UV light [18]. Zheng et al. showed that amylose/HNT/TiO$_2$ and HNT/TiO$_2$ nanocomposites (fabricated by ball milling and sol–gel synthesis) have excellent catalytic activity and good stability for the removal of methylene blue under UV irradiation [19].
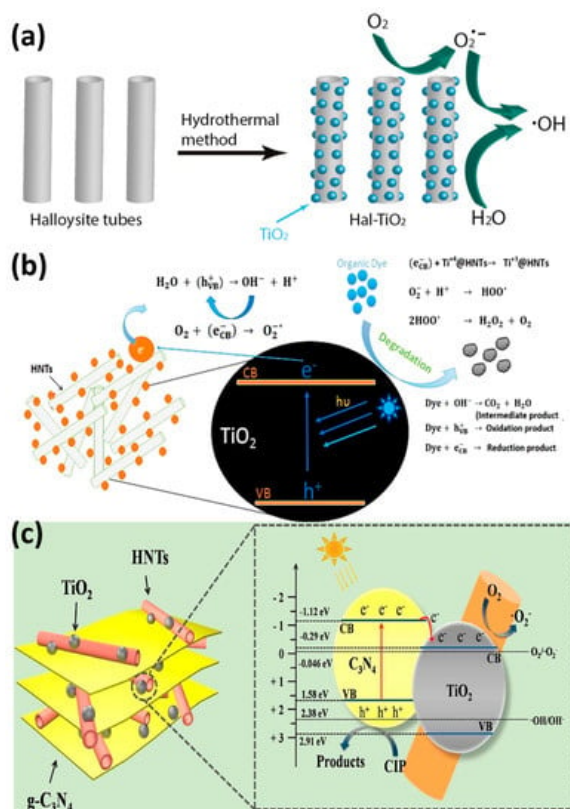

Figure 2. Schematic illustration of the production of the TiO$_2$/HNT photocatalyst [15] (**a**). Schematic description of the photocatalytic activity of TiO$_2$@HNT [18] (**b**). Ciprofloxacin (CIP) degradation in the presence of g-C$_3$N$_4$/TiO$_2$/HNT [20] (**c**).

Pharmaceutical compounds, such as painkillers, anti-inflammatory drugs, antibiotics, and hormones, are discharged into sewage treatment plants and are detected in surface water, groundwater, and drinking water due to their incomplete elimination. Wu et al. evaluated new hetero-structural g-C$_3$N$_4$/TiO$_2$/commercial halloysite composites (sol–gel and calcination at 500 °C) to eliminate ciprofloxacin from wastewater (**Figure 2**c). All composites (various mass ratios of melamine) displayed excellent photocatalytic activity under visible light and were stable. Particularly, the heterojunction composite eliminated 87% of ciprofloxacin in 60 min due to rapid photoelectron–hole pair transfer and separation [20]. Yu et al. prepared TiO$_2$-Hal nanocomposites by introducing fly-ash cenospheres into HNT, followed by rare earth ion imprinting. Then, they assessed their photocatalytic activity by monitoring the degradation of 40 mg/L tetracycline under visible light irradiation. The as-prepared photocatalyst modified by the functional monomer o-phenylenediamine had the highest photocatalytic activity (78.80% of tetracycline degraded in 50 min) [21]. Wang et al. synthesized Ce-doped TiO$_2$/HNT with a modified sol–gel method. By monitoring the photocatalytic degradation of tetracycline, they found that the photocatalytic performance of Ce-TiO$_2$/HNT was increased by approximately seven times compared with that of

TiO$_2$/HNT. This improvement was due to the reduction in the distance between the conduction and valence bands of TiO$_2$ by Ce doping [22].

Water contamination by pesticides from agricultural runoff entering nearby streams affects biodiversity, insects, birds, and other animal species. Szczepanik et al. used TiO$_2$-halloysite composites for degrading chloroaniline in water by photocatalysis. The nanocomposites were produced using titanium isopropoxide as a precursor and the hydrothermal method at 65 °C. The surface area and pore volume were increased in acid-activated halloysite samples. The photocatalytic performance of these nanocomposites for the degradation of aniline, 2-chloro, and 2,6-dichloroaniline under UV irradiation was improved compared with commercial Titania P25 [23]. Wang et al. showed that TiO$_2$/HNT (TiO$_2$ deposition on HNT surface by the one-step solvothermal method) (**Figure 3**a) displays a pH-sensitive degradation performance, with higher photocatalytic activity for acetic acid degradation [24]. Panagiotaras et al. were the first to investigate pesticide decomposition using TiO$_2$/HNT nanocomposites (fabricated with Hal nanotubes and the sol–gel method at 180 °C). They obtained the best performance with the halloysite-TiO$_2$ (10–90%) nanomaterial: 47.4% of tebuconazole (a fungicide) degradation under UV and visible light irradiation versus 33.2% for Titania P25F [25].
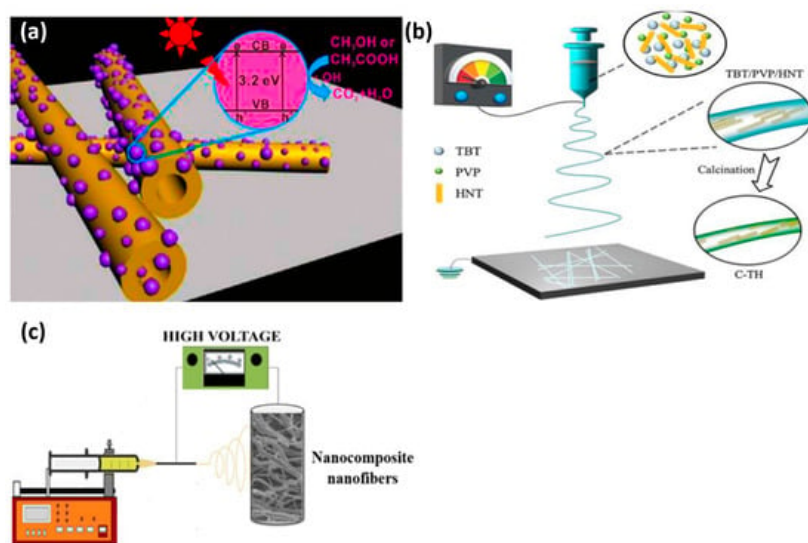

Figure 3. Photocatalytic process mediated by TiO$_2$ deposited on HNT [25] (**a**). Carbon/TiO$_2$/HNT hybrid nanofibers [26] (**b**). Illustration of the preparation of H95T5 nanofibers by combining halloysite and titanium oxide [4] (**c**).

Unlike the synthesis of TiO$_2$-decorated halloysite, the synthesis of TiO$_2$-HNT nanofibers is still in its infancy. Electrospinning is a simple method to produce nanofibers and fibers with different morphologies (e.g., hollow tubes, ribbons) [27] and with high production efficiency. Recently, Jiang et al. used the one-pot electrospinning/sol–gel method to fabricate carbon/TiO$_2$/HNT (**Figure 3**b). By monitoring methylene blue degradation under visible light, they showed that adding a modest HNT amount (8%) increases the degradation performance by 23 times compared with commercial TiO$_2$ anatase. This improvement was due to the improved mass transport of the reactant into the nanofibers [26]. Abid et al. used sol–gel and electrospinning to fabricate HNT-TiO$_2$ nanocomposites (**Figure 3**c) for the degradation of acetaminophen and methylene blue under UV and visible light. The nanocomposite, known as H95T5, which comprised 95% natural halloysite and 5% TiO$_2$, was able to degrade over 91% of acetaminophen and methylene blue after 150 and 360 min of exposure to visible light, respectively. They found that h$^+$ and O$_2^-$ played a major role in photocatalysis [4].

References

1. Fares, M.L.; Athmani, M.; Khelfaoui, Y.; Khettache, A. An investigation into the effects of conventional heat treatments on mechanical characteristics of new hot working tool steel. IOP Conf. Series Mater. Sci. Eng. 2012, 28, 012042.

2. Cheng, C.; Song, W.; Zhao, Q.; Zhang, H. Halloysite nanotubes in polymer science: Purification, characterization, modification and applications. Nanotechnol. Rev. 2020, 9, 323–344.

3. Ben Rhaiem, H.; Tessier, D.; Amara, A.B.H. Mineralogy of the <2 μm fraction of three mixed-layer clays from southern and central Tunisia. Clay Miner. 2000, 35, 375–381.

4. Abid, M.; Sayegh, S.; Iatsunskyi, I.; Coy, E.; Lesage, G.; Ramanavicius, A.; Amara, A.B.H.; Bechelany, M. Design of halloysite-based nanocomposites by electrospinning for water treatment. Colloids Surf. A Physicochem. Eng. Asp. 2022, 651, 129696.

5. Zhang, H.; Zhu, X.; Wu, Y.; Song, H.; Ba, X. High-efficiency grafting of halloysite nanotubes by using π-conjugated poly fluorenes via "click" chemistry. J. Mater. Sci. 2015, 50, 4387–4395.

6. Sakiewicz, P.; Lutynski, M.; Soltys, J.; Pytlinski, A. Purification of halloysite by magnetic separation. Physicochem. Probl. Miner. Process. 2016, 52, 991–1001.

7. Sakiewicz, P.; Lutynski, M.A. Purification of Dunino halloysite by H2SO4leaching and magnetic separation. E3S Web Conf. 2016, 8, 1032.

8. Rong, R.; Xu, X.; Zhu, S.; Li, B.; Wang, X.; Tang, K. Facile preparation of homogeneous and length controllable halloysite nanotubes by ultrasonic scission and uniform viscosity centrifugation. Chem. Eng. J. 2016, 291, 20–29.

9. Mohtor, N.H.; Othman, M.H.D.; Abu Bakar, S.; Kurniawan, T.A.; Dzinun, H.; Norddin, M.N.A.M.; Rajis, Z. Synthesis of nanostructured titanium dioxide layer onto kaolin hollow fibre membrane via hydrothermal method for decolourisation of reactive black 5. Chemosphere 2018, 208, 595–605.

10. Henych, J.; Štengl, V. Feasible Synthesis of TiO2 Deposited on Kaolin for Photocatalytic Applications. Clays Clay Miner. 2013, 61, 165–176.

11. Saad, E.M.; Elshaarawy, R.F.; Mahmoud, S.A.; El-Moselhy, K.M. New Ulva lactuca Algae Based Chitosan Bio-composites for Bioremediation of Cd(II) Ions. J. Bioresour. Bioprod. 2021, 6, 223–242.

12. Obey, G.; Adelaide, M.; Ramaraj, R. Biochar derived from non-customized matamba fruit shell as an adsorbent for wastewater treatment. J. Bioresour. Bioprod. 2022, 7, 109–115.

13. Du, Y.; Zheng, P. Adsorption and photodegradation of methylene blue on TiO2-halloysite adsorbents. Korean J. Chem. Eng. 2014, 31, 2051–2056.

14. Rapsomanikis, A.; Papoulis, D.; Panagiotaras, D.; Kaplani, E.; Stathatos, E. Nanocrystalline TiO2 and Halloysite clay mineral composite films prepared by sol-gel method: Synergistic effect and the case of silver modification to the photocatalytic degradation of Basic Blue- 41 azo dye in water. Glob. Nest J. 2014, 16, 485–498.

15. Papoulis, D.; Panagiotaras, D.; Tsigrou, P.; Christoforidis, K.; Petit, C.; Apostolopoulou, A.; Stathatos, E.; Komarneni, S.; Koukouvelas, I. Halloysite and sepiolite –TiO2 nanocomposites: Synthesis characterization and photocatalytic activity in three aquatic wastes. Mater. Sci. Semicond. Process. 2018, 85, 1–8.

16. Yao, P.; Zhong, S.; Shen, Z. TiO2/Halloysite Composites Codoped with Carbon and Nitrogen from Melamine and Their Enhanced Solar-Light-Driven Photocatalytic Performance. Int. J. Photoenergy 2015, 2015, 605690.

17. Li, C.; Wang, J.; Guo, H.; Ding, S. Low temperature synthesis of polyaniline–crystalline TiO2–halloysite composite nanotubes with enhanced visible light photocatalytic activity. J. Colloid Interface Sci. 2015, 458, 1–13.

18. Mishra, G.; Mukhopadhyay, M. TiO2 decorated functionalized halloysite nanotubes (TiO2@HNTs) and photocatalytic PVC membranes synthesis, characterization and its application in water treatment. Sci. Rep. 2019, 9, 4345.

19. Zheng, P.; Du, Y.; Chang, P.R.; Ma, X. Amylose–halloysite–TiO2 composites: Preparation, characterization and photodegradation. Appl. Surf. Sci. 2015, 329, 256–261.

20. Wu, D.; Li, J.; Guan, J.; Liu, C.; Zhao, X.; Zhu, Z.; Ma, C.; Huo, P.; Li, C.; Yan, Y. Improved photoelectric performance via fabricated heterojunction g-C3N4/TiO2/HNTs loaded photocatalysts for photodegradation of ciprofloxacin. J. Ind. Eng. Chem. 2018, 64, 206–218.

21. Yu, X.; Lu, Z.; Si, N.; Zhou, W.; Chen, T.; Gao, X.; Song, M.; Yan, Y.; Huo, P.; Yan, C. Preparation of rare earth metal ion/TiO2Hal-conducting polymers by ions imprinting technique and its photodegradation property on tetracycline. Appl. Clay Sci. 2014, 99, 125–130.

22. Wang, H.; Wu, D.; Li, X.; Huo, P. Ce doping TiO2/halloysite nanotubes photocatalyst for enhanced electrons transfer and photocatalytic degradation of Tetracycline. J. Mater. Sci. Mater. Electron. 2019, 30, 19126–19136.

23. Szczepanik, B.; Rogala, P.; Słomkiewicz, P.M.; Banaś, D.; Kubala-Kukuś, A.; Stabrawa, I. Synthesis, characterization and photocatalytic activity of TiO2-halloysite and Fe2O3-halloysite nanocomposites for photodegradation of chloroanilines in water. Appl. Clay Sci. 2017, 149, 118–126.

24. Wang, R.; Jiang, G.; Ding, Y.; Wang, Y.; Sun, X.; Wang, X.; Chen, W. Photocatalytic Activity of Heterostructures Based on TiO2 and Halloysite Nanotubes. ACS Appl. Mater. Interfaces 2011, 3, 4154–4158.

25. Bekiari, V.; Stathatos, E.; Papoulis, D.; Panagopoulos, G.; Kalarakis, A.; Iliopoulos, I.; Kourkouta, E.; Mavrokota, P. Use of halloysite–TiO2 nanocomposites for the decomposition of tebuconazole fungicide in water. Desalin. Water Treat. 2018, 127, 132–139.

26. Jiang, L.; Huang, Y.; Liu, T. Enhanced visible-light photocatalytic performance of electrospun carbon-doped TiO2/halloysite nanotube hybrid nanofibers. J. Colloid Interface Sci. 2015, 439, 62–68.

27. Chen, J.; Liao, W.; Jiang, Y.; Yu, D.; Zou, M.; Zhu, H.; Zhang, M.; Du, M. Facile Fabrication of ZnO/TiO2 Heterogeneous Nanofibres and Their Photocatalytic Behaviour and Mechanism towards Rhodamine B. Nanomater. Nanotechnol. 2016, 6, 9.